

Cross-shell excitations in doubly magic ^{132}Sn and its nearest neighbours

Sangeeta Das¹ and M. Saha Sarkar^{1,*}

¹*Saha Institute of Nuclear Physics, HBNI, Kolkata-700 064, India*

(Dated: May 20, 2020)

Large scale shell model calculations have been performed to study the excitation spectra of ^{132}Sn and its nearest neighbours with a new cross-shell interaction constructed from two widely used interactions, *sn100pn* and *CWG*, of this mass region. A few of the two-body matrix elements have been tuned to reproduce the low-lying multiplet states of ^{132}Sn . This is the first full scale shell model study of ^{132}Sn energy spectra as well as transition probabilities. The excitation spectra for other nearest neighbours are reproduced reasonably well. The most important observable calculated are the E1 transition probabilities, which were so far beyond the scope of calculations with the existing interactions.

PACS numbers: 21.60.Cs, 23.20.Lv, 23.20.-g, 27.60.+j

I. INTRODUCTION

Nuclei near doubly closed shell nuclei, act as testing ground of different nuclear models. Their excitation spectra [1] typically show an admixture of two different modes of excitation. One mode arises from the excitation of valence particles within the shell and the other involves excitations across the shell gaps, which are especially important at higher excitation energies.

In general, to describe the low energy states, different effective interactions are used, involving at best an intruder orbital from the higher opposite parity shell. The high energy states involving cross-shell excitations warrant the inclusion of other orbitals across the shell. However, such interactions involving cross-shell excitation possibilities are usually not available for heavy nuclei, apart from a few recent ones [2]. Moreover, unrestricted calculations over such large valence space encompassing two major shells are mostly computationally challenging - thus, suitable truncation schemes are adopted.

The nuclei around the doubly magic ^{132}Sn in $A \simeq 130$ mass region play a significant role in both nuclear structure physics and nuclear astrophysics. Thus this region has drawn the attention of experimentalists as well as theoreticians. Two different model spaces for neutrons are adopted to study the nuclei with neutron number $N < 82$ and $N > 82$. The active neutron orbits in them are

- for $N < 82$, the neutron as well as proton model spaces consist of the five orbits ($1g_{7/2}$, $2d_{5/2}$, $2d_{3/2}$, $3s_{1/2}$ and $1h_{11/2}$) above ^{100}Sn core with $Z, N=50$.
- for $N > 82$, the neutron model space includes six orbits, *viz.*, ($1h_{9/2}$, $2f_{7/2}$, $3p_{3/2}$, $3p_{1/2}$, $2f_{5/2}$, and $1i_{13/2}$), with proton model space same as above, with $Z=50$ and $N=82$, i.e. ^{132}Sn as the core.

The effective interactions *sn100pn* and *CWG*, discussed in detail in Ref. [3], are obtained starting with

a G matrix derived from the CD-Bonn nucleon-nucleon interaction. They are widely used and are successful in explaining the low energy states. However, they are unable to explain states at higher energies which involve cross-shell excitations. These interactions fail to explain the excitation spectra of a doubly closed shell nucleus, like, ^{132}Sn and only its ground state can be calculated. Even for its very close neighbours, only a few low energy states can be determined theoretically. These interactions are quite successful in reproducing the excitation spectra, transition probabilities and moments of other nuclei. However, they fail to reproduce transition probability of hindered E1 transitions, because of the limitation in the valence space. There are no opposite parity orbitals in their model spaces with $\Delta I = 1$ to generate non-zero E1 transition density.

However, E1 transitions are frequently observed in these nuclei and play important roles in their low lying spectra. Not only in regions near the shell closures, but also at the mid-shell (near ^{118}Sn) region E1 transitions are observed as decay-out transitions of isomers [1].

In the present work, we have derived a new effective interaction in an extended basis space including most of the neutron orbits from two major shells. The new interaction has been formulated to remove the limitations of the existing interactions. The applicability of the interaction has been tested by calculating binding energies, excitation spectra and electromagnetic transition probabilities of ^{132}Sn and its close neighbours.

II. DERIVATION OF THE EFFECTIVE INTERACTION AND CALCULATIONS

In this section, we shall describe the derivation of the new interaction, which will be referred to as *sm56* with appropriate suffixes for different variant interactions, like *sm56fp* and *sm56fph*.

*maitrayee.sahasarkar@saha.ac.in

A. Model space and choice of single particle energies (*spe*)

The model space consists of two proton (π) orbitals ($\pi 1g_{7/2}$ and $\pi 2d_{5/2}$) and eight neutron (ν) orbitals ($\nu 1g_{7/2}$ and $\nu 2d_{5/2}$, $\nu 2d_{3/2}$, $\nu 3s_{1/2}$, $\nu 1h_{11/2}$, $\nu 1h_{9/2}$, $\nu 2f_{7/2}$, $\nu 3p_{3/2}$) with ^{100}Sn as core.

The present Hamiltonian has been constructed from two very well known interactions of this region: *sn100pn* and *CWG* interactions [3]. For the sake of clarity in explaining this new interaction, the proton orbits are denoted by P and the neutron orbits below $N = 82$ shell ($1g_{7/2}$, $2d_{5/2}$, $2d_{3/2}$, $3s_{1/2}$, $1h_{11/2}$) are expressed as N1 and those above $N = 82$ shell ($1h_{9/2}$, $2f_{7/2}$, $3p_{3/2}$) are referred to as N2.

The proton single particle energies (*spe*) are 0.8072 and 1.5623 MeV for $\pi 1g_{7/2}$ and $\pi 2d_{5/2}$ orbits.

The neutron single particle energies (*spe*) are taken as -9.74, -8.97, -7.31, -7.62, -7.38 MeV for the orbits below $N = 82$ shell closure, *viz.*, $\nu 1g_{7/2}$, $\nu 2d_{5/2}$, $\nu 2d_{3/2}$, $\nu 3s_{1/2}$, $\nu 1h_{11/2}$, respectively, as suggested in Ref. [3]. These *spes* are chosen such that they reproduce the experimental levels of ^{131}Sn [3].

For the orbitals above $N = 82$ shell, we have adjusted the neutron *spes*. We have reproduced the experimental binding energy (*be*) of ^{133}Sn with respect to ^{132}Sn by adjusting the *spe* of $\nu 2f_{7/2}$ orbit. All the orbitals below $N = 82$ shell are filled up and only one particle is allowed to be in the orbit above $N = 82$ shell to reproduce the ground - state *be*, and excitation energies of $3/2_1^-$ and $9/2_1^-$ states of ^{133}Sn . The *spes* thus chosen are 11.06, 5.718, 8.287 MeV for $\nu 1h_{9/2}$, $\nu 2f_{7/2}$, $\nu 3p_{3/2}$ orbits, respectively.

B. The two body matrix elements (*tbmes*)

The two-body matrix elements (*tbme*) are constructed in the following way.

- The proton-proton *tbmes*, $\langle P_i P_j | V | P_k P_l \rangle_{I,1}$ where i,j,k,l are proton orbits $\pi 1g_{7/2}$ and $\pi 2d_{5/2}$ coupled to total angular momentum I and isospin $T=1$, are taken from *sn100pp* ($\pi - \pi$ part of *sn100pn* interaction) including the Coulomb terms (*sn100co*).
- The neutron-neutron *tbmes* are been divided in a few groups. They are
 - The *tbmes* of the intra-shell interaction for orbits below $N = 82$ shell, $\langle N1_i N1_j | V | N1_k N1_l \rangle_{I,1}$ (i.e for $\nu 1g_{7/2}$, $\nu 2d_{5/2}$, $\nu 2d_{3/2}$, $\nu 3s_{1/2}$, $\nu 1h_{11/2}$) coupled to I and $T=1$, are obtained from *sn100nn* interaction.
 - For $N > 82$, $\langle N2_i N2_j | V | N2_k N2_l \rangle_{I,1}$ *tbmes* (i.e. interaction between $\nu 1h_{9/2}$, $\nu 2f_{7/2}$, $\nu 3p_{3/2}$) coupled to I and $T=1$, have been taken from *CWG* interaction.
 - The $T = 1$, $\pi - \nu$ *tbmes* of *CWG* interaction have been taken as cross-shell neutron-neutron *tbmes*, *viz.*, $\langle N1_i N2_j | V | N1_k N2_l \rangle_{I,1}$ keeping in mind the

charge independence and isospin invariance of nuclear interaction.

- The rest of neutron-neutron *tbmes* like $\langle N1_i N2_j | V | N1_k N1_l \rangle_{I,1}$ or $\langle N1_i N2_j | V | N2_k N2_l \rangle_{I,1}$, which are not present in the $\pi - \nu$ *tbme* set of *CWG* interaction have been calculated from zero range delta interaction [4].
- The proton-neutron *tbmes* for neutron orbits below $N=82$, *viz.*, $\langle P_i N1_j | V | P_k N1_l \rangle_{I,1}$ and 0 have been considered from *sn100pn* and those for ν orbits above $N = 82$ shell, *viz.*, $\langle P_i N2_j | V | P_k N2_l \rangle_{I,1}$ and 0 have been taken from *CWG* interaction.
- Rest of the $\pi - \nu$ *tbmes*, *viz.*, $\langle P_i N1_j | V | P_k N2_l \rangle_{I,1}$ and 0 have been calculated from delta interaction as discussed above.

1. Tuning of cross-shell $\nu - \nu$ *tbmes*

However, the set of cross-shell $\nu - \nu$ *tbmes* of particle-hole multiplets, which are obtained from the $T=1$ *tbmes* of $\nu - \pi$ interaction from *CWG* Hamiltonian can not reproduce the low-lying experimental spectra of ^{132}Sn [5]. These states are identified by earlier workers [6] as members of particle-hole multiplets from theoretical calculations using Random Phase Approximation (RPA).

This failure of the collated interaction is not unexpected. Although the nuclear interaction is charge independent - the requirement of Pauli exclusion principle which warrants anti-symmetrization of the two-nucleon wave function, distinguishes the interaction between like nucleons from that arising between unlike nucleons. It is found that although the interaction energies of $T=1$ parts of $\nu - \nu$, $\nu - \pi$ and $\pi - \pi$ are alike for a pair of nucleons in the same orbit, the monopole interaction between like nucleons is weaker than those between unlike ones [7]. For dissimilar orbits, the interaction energies are grossly different. For two unlike nucleons, the monopole interaction is attractive. However, for like nucleons, it is mainly repulsive.

Thus to tune the $\nu - \nu$ *tbmes* of important and relevant multiplets for ^{132}Sn , the procedure described in Ref. [7] has been followed. The experimental binding energies of ^{131}Sn , ^{132}Sn and ^{133}Sn from Ref. [8] and the experimental excitation energies of multiplet states are utilized to get the diagonal *tbmes* of corresponding multiplets.

- *The low-lying positive parity states in ^{132}Sn :*

The two cross-shell positive parity multiplets which are of utmost importance in the low-lying spectra of ^{132}Sn arise from couplings of $1h_{11/2}^{-1} - 2f_{7/2}$ [6] and $1h_{11/2}^{-1} - 3p_{3/2}$ orbitals. The coupling of $1h_{11/2}^{-1} - 1h_{9/2}$ orbits has been the most significant for the generation of 8_2^+ state.

– The $\nu 1h_{11/2}^{-1} - \nu 2f_{7/2}$ *tbmes* :

The experimental binding energies of ^{131}Sn , ^{132}Sn and ^{133}Sn from Ref. [8] and the experimental excitation energies of ^{132}Sn (2_1^+ , 4_1^+ , 5_1^+ , 6_1^+ , 7_1^+ , 8_1^+ , 9_1^+ , which are considered to be members of $1h_{11/2}^{-1} - 2f_{7/2}$ multiplet [6]) are utilized to get the diagonal *tbmes* of $1h_{11/2}^{-1} - 2f_{7/2}$ coupling. Since the minimum angular momentum generated by this coupling is 2, the $E_x(2^+) = 4.041$ MeV is used as reference energy. Most of the *tbmes* are negative and thus the interaction is attractive (Fig.1). The monopole contribution to the interaction energies is denoted by the dashed line in the figure. The adopted experimental level scheme of ^{132}Sn does not include a 3^+ state, thus the corresponding interaction energy has not been modified. The Fig. 1 shows comparison of the $\pi - \nu$ interaction energies from *CWG* interaction [3] with the present modified ones for $\nu - \nu$. Similar to the observation in Ref. [7], for $1h_{11/2}^{-1} - 2f_{7/2}$ coupling, the monopole interaction between neutrons (-0.1374 MeV) is about two times less attractive than those between neutron-protons (-0.2317 MeV).

– Tuning of $\nu 1h_{11/2}^{-1} - \nu 3p_{3/2}$:

The $\nu 1h_{11/2}^{-1} - \nu 3p_{3/2}$ coupling can generate angular momenta 4^+ to 7^+ . At the low spins, experimental level scheme of ^{132}Sn , only two 6^+ and 7^+ are reported. Unlike those for $\nu 1h_{11/2}^{-1} - \nu 2f_{7/2}$ coupling, all *tbmes* corresponding to $\nu 1h_{11/2}^{-1}$ coupled with $\nu 3p_{3/2}$ could not be determined systematically, due to lack of experimental data. However, only two relevant *tbmes* are tuned to improve the predictions for second 6^+ and 7^+ states.

– Tuning of $\nu 1h_{11/2}^{-1} - \nu 1h_{9/2}$ *tbmes*:

Similar situation prevails for tuning the *tbmes* of the coupling of $\nu 1h_{11/2}^{-1} - \nu 1h_{9/2}$, which can generate angular momenta 1^+ to 10^+ . Relevant two *tbmes* for this coupling have been tuned to improve the predictions for second 7^+ and 8^+ states.

• The low-lying negative parity states in ^{132}Sn :

The negative parity 3_1^- , 4_1^- and 5_1^- states do not have pure multiplet structure. These angular momenta can be generated from the coupling of $\nu 2d_{3/2}^{-1}$ and $\nu 2f_{7/2}$. The 3_1^- , 4_1^- states also have contributions from the $\nu 3s_{1/2}^{-1}$ coupled with $\nu 2f_{7/2}$. The holes in $\nu 2d_{5/2}$ and $\nu 1g_{7/2}$ can couple with $\nu 2f_{7/2}$, to generate these negative parity states. Thus these matrix elements are not modified.

2. Tuning of inter-shell *tbmes*

The new modified interaction does not include the full proton model space as considered in *sn100pp* and *CWG* interactions. The neutron model space for $N > 82$ has also

been truncated from the one used in *CWG* Hamiltonian. Thus the corresponding $\pi - \pi$ and $\nu - \nu$ *tbmes* of the truncated spaces are modified.

• The $\pi - \pi$ *tbmes*:

The diagonal two body matrix element for $\pi 1g_{7/2} - \pi 1g_{7/2}$ coupled to $I=0$ is adjusted to reproduce the binding energy of ^{134}Te .

• The $\nu - \nu$ *tbmes*:

The $\nu 2f_{7/2} - \nu 2f_{7/2}$ *tbmes* are adjusted to reproduce the binding energy and excitation energies of 2_1^+ to 6_1^+ levels of ^{134}Sn . The $\nu 2f_{7/2} - \nu 1h_{9/2}$ *tbme* corresponding to $I=8^+$ has been adjusted to reproduce the experimental 8_1^+ excitation energy.

C. The interactions

Two versions of the interaction have been generated. The first one, named as *sm56fp* includes only the modifications in $\nu - \nu$ *tbmes* (except those corresponding to $\nu 1h_{11/2}^{-1} - \nu 1h_{9/2}$) of the collated interaction. The final version of the interaction which includes all modifications in $\nu - \nu$ and $\pi - \pi$ *tbmes* as discussed above, is named as *sm56fph*.

D. The calculations

The shell-model code NUSHELLX@MSU [9] and OXBASH [10] are used for the calculations using the interactions discussed above. The excitation spectra as well as transition probabilities (including $B(E1)$ values) of ^{132}Sn have been calculated and compared with experimental data. The predictability of our shell-model Hamiltonian in the neighbourhood of ^{132}Sn has also been tested. The excitation spectra of a few nuclei around ^{132}Sn with neutron numbers 81 - 83 are calculated. They are $^{131,132}_{50}\text{Sn}_{81,84}$, $^{132-134}_{51}\text{Sb}_{81-83}$, $^{133-135}_{52}\text{Te}_{81-83}$ and $^{135}_{53}\text{I}_{82}$. The excitation spectra of these nuclei have been calculated with no restriction of neutrons for $N < 82$ orbitals. For nuclei with $N \leq 82$ neutrons, allowed excitation modes considered are: (i) no neutron (0p0h) beyond $N > 82$ orbits, or, (ii) at least one neutron excited in any of the three orbits (1p1h), (ii) 2p2h and (iii) maximum one neutron excited in each of the three orbits (3p3h). Thus from no neutron in $N > 82$ orbits, 1p1h to 3p3h excitations in these orbits are possible in this choice. For nuclei with $N > 82$, apart from the neutrons already in $N > 82$ orbitals, 1p1h to 3p3h excitations are allowed. However, in some of the cases discussed below, such options were not computationally feasible with our facilities. Thus we had to restrict to 2p2h or even 1p1h excitations only. A chart (Fig. 2) shows the nuclei for which theoretical calculations have been done. The maximum *nprh* excitation mode which was computationally possible in the present calculation is also indicated for each nucleus in the chart.

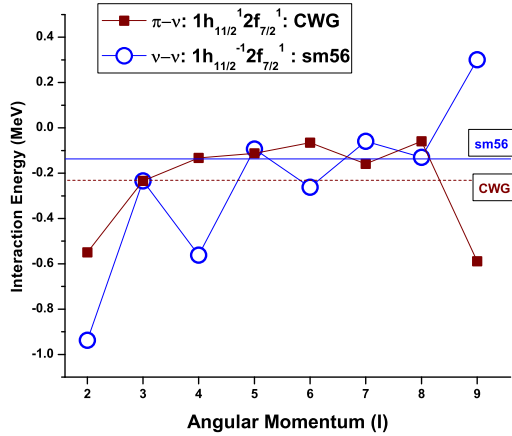


FIG. 1: Empirical interaction energy between two nucleons. One of them is in $1h_{11/2}$ and other in $2f_{7/2}$ orbit. The *CWG* (*sm56*) *tbmes* are for $\pi - \nu$ ($\nu - \nu$) interaction. The dashed (solid) line indicates the monopole energy for *CWG* (*sm56*) interaction.

Z = 53		^{135}I 2p2h	
Z = 52	^{133}Te 1p1h	^{134}Te 2p2h	^{135}Te 1p1h
Z = 51	^{132}Sb 2p2h	^{133}Sb 2p2h	^{134}Sb 2p2h
Z = 50	^{131}Sn 3p3h	^{132}Sn 3p3h	
	N = 81	N = 82	N = 83

FIG. 2: List of nuclei for which theoretical calculations have been done. The maximum npnh excitation mode which was computationally possible in the present calculation has been indicated in the chart.

III. RESULTS AND DISCUSSION

A. Binding Energies

The trend in the calculated binding energies in 1p1h option for neutrons (where maximum one neutron can be excited to any one of the orbits above $N=82$ and no restriction in the orbits below $N=82$) with respect to that of ^{132}Sn are reproduced well in theory (Fig. 3). The values are plotted for isotones of Sn to I for $N=80$ to 84 . The excitation spectra of these nuclei have been calcu-

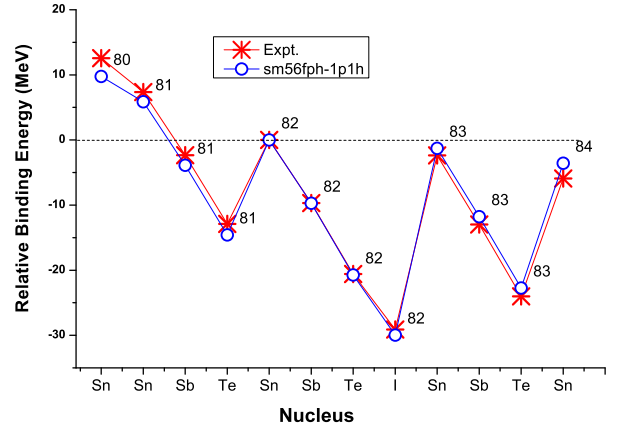


FIG. 3: Comparison of calculated and experimental binding energies with respect to ^{132}Sn .

lated with the *sm56fph* interaction.

B. Excitation Energies

• Calculations for $N=82$ isotones

1. $^{132}_{50}\text{Sn}_{82}$

The excitation spectra of ^{132}Sn has been calculated with no restriction of neutrons for $N < 82$ orbitals with at best one particle excited in each of the three orbits for $N > 82$. Thus from no neutron in $N > 82$ orbits, 1p1h to 3p3h excitations in these orbits are allowed.

The doubly closed shell ^{132}Sn with $Z=50$ and $N=82$, has its first excited state, 2^+ at relatively higher energy (~ 4 MeV) than its neighbouring nuclei due the excitation of neutrons across the $N=82$ shell closure. Thus, the low lying excited states of this doubly closed shell nucleus can be explained by particle-hole (p-h) excitations. As the excitations involve only a few particle and hole states, the structure of individual states should possess nearly pure multiplet structure.

P. Bhattacharyya *et al.* [5] have identified the first 2^+ , 4^+ , 5^+ , 6^+ , 7^+ , 8^+ , 9^+ states as members of $\nu 1h_{11/2}^{-1}2f_{7/2}$ multiplet. In the present work, the interaction has been tuned as discussed in Sec. II. The theoretical results from 3p3h excitation modes with *sm56fp* and *sm56fph* interactions show similar agreement with experimental data in Fig. 4, except for the 8^+_{2-} state.

Fogelberg *et al.* [11] have described the positive parity 6^+_{2-} , 8^+_{2-} , and 7^+_{2-} states near 5.4 MeV as members of $\pi 1g_{9/2}^{-1}1g_{7/2}$ multiplet. The $\pi 1g_{9/2}$ orbital is not included in our valence space. However, in the

present calculation, 6_2^+ , and 7_2^+ are reproduced well with *sm56fp* and they originate from $\nu 1h_{11/2}^{-1}2p_{3/2}$ multiplet. The 8_2^+ corresponding to $\nu 1h_{11/2}^{-1}1h_{9/2}$ multiplet shows gross mismatch with experiment for results with *sm56fp* interaction. In the *sm56fph*, the corresponding *tbmes* relevant for 6_2^+ , 8_2^+ , and 7_2^+ states are tuned to reproduce them. Thus, with *sm56fph* interaction, experimental energies of these states are reproduced much better (Fig. 4).

The level at 4.352 MeV is identified as a 3_1^- state in the study by B. Fogelberg *et al.* [11]. It is expected that the lowest 3_1^- , 4_1^- and 5_1^- states originate from the coupling of $\nu 2d_{3/2}^{-1}2f_{7/2}$. Theoretically calculated energies of 4_1^- and 5_1^- states match with experimental data within 100-200 keV for *sm56fph* interaction, without any tuning of the relevant *tbmes*, the 3_1^- state is over predicted by $\simeq 600\text{keV}$. However, 4_1^- originates from the partition $\nu 2d_{3/2}^{-1}2f_{7/2}$ (96%), 5_1^- has 88% contribution from $\nu 2d_{3/2}^{-1}1h_{9/2}$. The 5_2^- calculated at 5.299 MeV is a member of the $\nu 2d_{3/2}^{-1}2f_{7/2}$ multiplet. The inability of shell model theory to reproduce the energy of 3_1^- state has been also discussed in Ref. [11]. They have argued that the 3_1^- and 5_1^- levels of ^{132}Sn should be present within about 100 keV from each other. The experimental energy of the 5_1^- level is 4.942 MeV. The experimental energy of 3_1^- is around 600 keV lower than the other members of the $\nu 2d_{3/2}^{-1}2f_{7/2}$ multiplet. This is a signature of the collective nature of this state - which is generated from a coherent superposition of many p-h configurations. The failure of the present calculation (to be discussed in Sec. III C) to reproduce the enhanced E3 transition from this state also supports the possible collective nature of this state.

The 6_1^- state which originates from the partition $\nu 2d_{3/2}^{-1}1h_{9/2}$ is also underpredicted in theory. However, 6_2^- , 6_3^- and 7_1^- states originated primarily from $\nu 2d_{5/2}^{-1}2f_{7/2}$ (99%), $\nu 2d_{5/2}^{-1}1h_{9/2}$ (98%) and $\nu 2d_{5/2}^{-1}1h_{9/2}$ (95%) partitions, respectively, are reproduced well in theory.

2. $^{133}\text{Sb}_{82}$

The immediate neighbour of ^{132}Sn , ^{133}Sb with a proton coupled with the doubly closed shell nucleus, provides excellent opportunity to study the single proton states beyond $Z=50$. Its relatively higher spin, low excitation energy spectra primarily involve neutron p-h excitation across the shell gap at $N=82$. Several experimental groups [12–16] have worked to extract experimental data for ^{133}Sb . A high-spin isomer arising from core-excitation was identified by them. At GSI, using isochronous mass spectrometry, the core excited isomeric state was first directly identified at an excitation energy of 4.56(10) MeV with measured half-life of

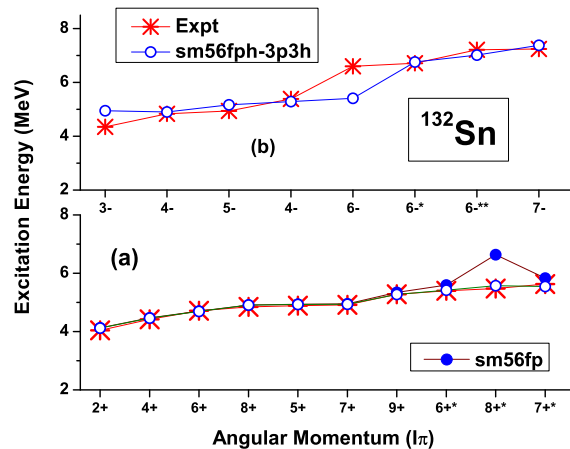


FIG. 4: (Color Online) Comparison of (a) positive parity and (b) negative parity states in the experimental spectra of ^{132}Sn with theory with 3p3h excitations. The results with *sm56fp* are shown with filled blue bullets and those with *sm56fph* are indicated with open blue bullets. The number of asterisks (N) appearing as superscript in the value of angular momentum in the x-axis label indicate it as the (N+1)th state of that spin.

$17\ \mu\text{s}$ [17]. They have also provided a limiting value of the half-life for the fully ionized ^{133}Sb nuclei corresponding to a totally disabled internal conversion decay mode. Information about the core-excited states of ^{133}Sb above $21/2^+$ state has been obtained later, from cold neutron induced fission of ^{241}Pu and ^{235}U in an experiment performed at ILL reactor in Grenoble [6]. The property of these core excited states, offer an opportunity to test the newly formulated shell model interaction.

The spectra of ^{133}Sb are calculated with both 1p1h and 2p2h excitation options with *sm56fph* interaction. No restriction has been put for neutrons in the $N < 82$ orbitals. Results for both 1p1h as well as 2p2h are shown in the Fig. 5. The 3p3h excitations could not be included in the calculations due to computational limitation.

In our calculation, $3/2^+$ and $11/2^-$ at the energy 2.44 MeV and 2.792 MeV are not reproduced. These are originated from the single proton excitation to $\pi 2d_{3/2}$ and $\pi 1h_{11/2}$ orbitals, which are not included in the present model space. Thus these states are not included in the Fig. 5.

However, the higher energy (> 4 MeV) positive and negative parity states arising from core-excitation are reproduced quite well (Fig. 5) in 2p2h excitation mode. Similar to ^{132}Sn , the positive parity $11/2_1^+$, $13/2_1^+$, $15/2_1^+$, $17/2_1^+$ and $21/2_1^+$ states originate primarily from the partition $\nu 1h_{11/2}^{-1}2f_{7/2}$ coupled with $\pi 1g_{7/2}$ with 90-94% contribution in their wavefunctions. The $21/2_2^+$, $23/2_1^+$ and $25/2_1^+$ have contribution (96%, 89%

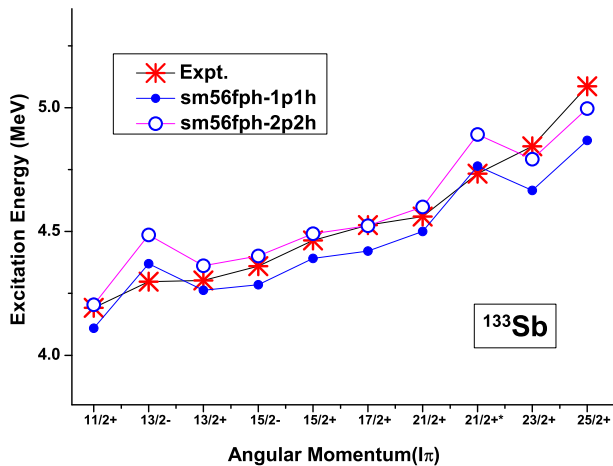


FIG. 5: Comparison of experimental spectra of high spin states in ^{133}Sb with theory. More details are included in the legend, caption of Fig. 4 and the text.

and 97%) from the partition $\nu 1h_{11/2}^{-1}1h_{9/2}$ coupled with $\pi 1g_{7/2}$.

The negative parity $13/2_1^-$ and $15/2_1^-$ states have 86% and 70% contributions from the partition $\nu 2d_{3/2}^{-1}2f_{7/2}$ coupled with $\pi 1g_{7/2}$. The 2p2h option successfully reproduce experimental data except for $13/2_1^-$ and $21/2_2^+$ states, where 1p1h option is in better agreement.

3. $^{134}\text{Te}_{82}$

^{134}Te contains two valence protons outside the ^{132}Sn core. Most of the experimental data have been obtained from coincidence measurement of prompt and delayed gamma ray cascades of fission fragments emitted following spontaneous fission using large γ -detector arrays [18–22].

At low excitations (upto $\simeq 3$ MeV), the states mainly originate from proton excitations within the shell. The two most important partitions are $\pi 1g_{7/2}^2$ and $\pi 1g_{7/2} - 2d_{5/2}$. Results from the present work with 2p2h excitations match quite well with experimental data even for these low spins (Fig. 6).

Above 3 MeV (but < 4.5 MeV), few negative parity states are observed and these are expected to originate from the multiplets of $\pi 1g_{7/2}1h_{11/2}$. These negative parity states were not reproduced. The present model space does not include $\pi 1h_{11/2}$ orbit. Thus a neutron has to be excited beyond the shell gap, to produce a negative parity state, which resulted in the higher excitation energy. These states are not included in the Fig. 6.

The first one in the set of excited states involving excitations across the neutron core has been

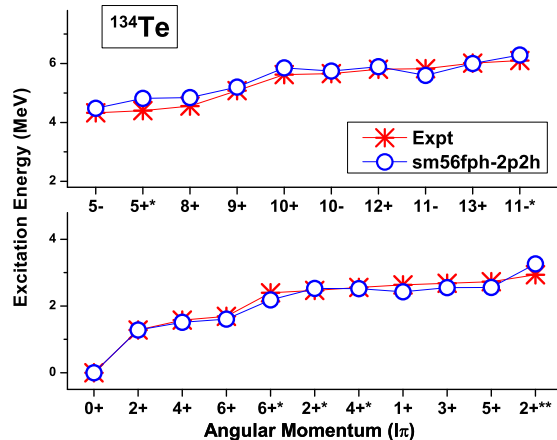


FIG. 6: Comparison of experimental spectra of ^{134}Te with theory. See legend, caption of Fig. 4 and text for more details.

identified at excitation energy 4.558 MeV [22] with $I^\pi=8^+$. These positive parity states are interpreted to be members of the multiplets of $\pi 1g_{7/2}^2 - \nu 1h_{11/2}^{-1}2f_{7/2}$. Results for 2p2h calculations are shown in the Fig. 6. In our calculation, 8_1^+ state at 4.843 MeV has this configuration with around 90% amplitude. Whereas, the 9_1^+ has nearly 70% contribution from $\pi 1g_{7/2}^2 - \nu 1h_{11/2}^{-1}1h_{9/2}$. The 10_1^+ state predicted at 5.85 MeV ($E_{\text{expt}}=5.621$ MeV), has a mixed configuration with $\pi 1g_{7/2}^2 - \nu 1h_{11/2}^{-1}2f_{7/2}$ ($\simeq 59\%$), $\pi 1g_{7/2}2d_{5/2} - \nu 1h_{11/2}^{-1}2f_{7/2}$ ($\simeq 36\%$). The yrast 12^+ (13^+) state have dominant contribution of $\simeq 45\%$ (31%) $\pi 1g_{7/2}^2 - \nu 1h_{11/2}^{-1}2f_{7/2}$ and $\simeq 48\%$ (65%) $\pi 1g_{7/2}2d_{5/2} - \nu 1h_{11/2}^{-1}2f_{7/2}$ partition.

The negative parity state 10_1^- ($E_{\text{expt}}=5.658$ MeV) at 5.746 MeV has mixed composition with 45% contribution from the partition $\pi 1g_{7/2}^2 - \nu 2d_{3/2}^{-1}2f_{7/2}$ and 24% from $\pi 1g_{7/2}2d_{5/2} - \nu 2d_{3/2}^{-1}2f_{7/2}$. The 11_1^- has 77% contribution from $\pi 1g_{7/2}^2 - \nu 2d_{3/2}^{-1}1h_{9/2}$ and 11_2^- on the other hand, has 72% contribution from the partition $\pi 1g_{7/2}2d_{5/2} - \nu 2d_{3/2}^{-1}1h_{9/2}$. Overall agreement with experimental data is reasonably good.

4. $^{135}\text{I}_{82}$

The experimental data about the excited states of this nucleus have been mainly obtained from the decay [23] of ^{135}Te and from the prompt γ -ray spectroscopy of the spontaneous fission fragments of ^{248}Cm [20, 22].

Three valence protons outside the $Z=50$ core dominate the low lying yrast excitations of this nucleus. The low lying states within 1.5 MeV ($7/2_1^+$, $9/2_1^+$, $11/2_1^+$,

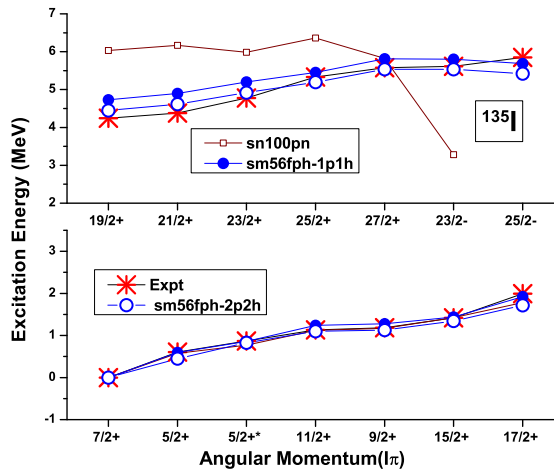


FIG. 7: Comparison of experimental spectra of ^{135}I with theory. More details are included in the legend, caption of Fig. 4 and the text.

$15/2_1^+$) have major contribution from $\pi 1g_{7/2}^3$. Theoretical results (Fig. 7) show good agreement with data. The $5/2_1^+$ and $17/2_1^+$ states on the other hand show dominant participation of $\pi 1g_{7/2}^2 2d_{5/2}$ partition. A few negative parity states are observed at excitation energies beyond 3.5 MeV but less than 4 MeV. These are expected to arise from the multiplets of $\pi 1g_{7/2}^2 1h_{11/2}$, which is beyond the scope of this calculation. Thus these states are not included in the Fig. 7.

The core excited states of ^{135}I have been observed after 4 MeV. Results with 1p1h excitations and 2p2h excitations for *sm56fph* interaction are shown in Fig. 7. The positive parity states ($19/2_1^+$, $21/2_1^+$, and $23/2_1^+$) are reproduced better with 2p2h excitations. The $19/2_1^+$, $21/2_1^+$ states have $\simeq 55\%$ and 42% (57% and 45%) contributions from $\pi 1g_{7/2}^2 2d_{5/2} - \nu 1h_{11/2}^{-1} 2f_{7/2}$ and $\simeq 36\%$ and 48% (35% and 46%) from $\pi 1g_{7/2}^3 - \nu 1h_{11/2}^{-1} 2f_{7/2}$ partitions with 2p2h (1p1h) modes. For $23/2_1^+$, both the modes of excitations predict $\simeq 75\%$ contribution from $\pi 1g_{7/2}^3 - \nu 1h_{11/2}^{-1} 2f_{7/2}$ partition. Both the modes predict $25/2_1^+$ with a deviation of around 130 keV. They have common dominant structure of $\pi 1g_{7/2}^3 - \nu 1h_{11/2}^{-1} 1h_{9/2}$ with $\simeq 83\%$ contributions. The Fig. 7 clearly shows the failure of *sn100pn* interaction to reproduce the core-excited states.

Core excited negative parity states $23/2_2^-$ ($25/2_1^-$) are observed after 5.7 MeV [22]. The negative parity state $23/2_2^-$ shows better agreement with theoretical prediction for 2p2h excitation. The composition of the state has $\simeq 53\%$ (50%) contribution from $\pi 1g_{7/2}^2 2d_{5/2} - \nu 2d_{3/2}^{-1} 2f_{7/2}$ for 1p1h (2p2h excitation). Experimentally observed $25/2^-$ state at energy at 5.849 MeV matches with $25/2_1^-$ state with $\simeq 67\%$ contribution

from $\pi 1g_{7/2}^2 2d_{5/2} - \nu 2d_{3/2}^{-1} 1h_{9/2}$ for 1p1h excitation. Whereas, 2p2h shows deviation around 400keV with $\simeq 57\%$ contribution from $\pi 1g_{7/2}^2 2d_{5/2} - \nu 2d_{3/2}^{-1} 2f_{7/2}$ partition.

- Calculations for $N=81$ isotones

5. $^{131}_{50}\text{Sn}_{81}$

This nucleus has a single neutron hole coupled to the doubly magic ^{132}Sn . Thus one can gain information about the single hole states, useful for nuclear shell model calculations in its structure. Experimentally, the single hole states ($1g_{7/2}$, $2d_{3/2}$, $3s_{1/2}$) in ^{131}Sn were studied from β -decay experiments by De Geer and Holm [24]. There is some uncertainty in the relative position of the $11/2_1^-$ state originated from one neutron hole in $1h_{11/2}$ orbit. This state is a β -decaying isomer. Several experiments have been performed to determine the energy of $11/2_1^-$ state precisely [25–27]. The most recently adopted data reports that the energy obtained from the β spectrum is 69 (14) keV, whereas it is 65.1 (3) keV from the level scheme [1]. This state is the first excited state of ^{131}Sn nucleus. Our calculations for 3p3h mode of excitation with *sm56fph* interaction predict this energy as 36 keV. The trend of other low-lying excited states $1/2_1^+$, $5/2_1^+$, $7/2_1^+$ at 0.332 MeV, 1.655 MeV, 2.434 MeV, respectively, as determined from the decay studies [24, 27] are reproduced in the calculated spectra (Fig. 8). However, the theoretical values do not exactly reproduce the experimental data for $1/2_1^+$ and $7/2_1^+$.

Higher excited states in the energy range 4-5 MeV populated from the spontaneous fission of ^{248}Cm were studied via prompt-delayed gamma spectroscopy [5]. The positive parity states $13/2_1^+$, $15/2_1^+$, $17/2_1^+$ and $19/2_1^+$ are found to be originated from the coupling of $\nu 2d_{3/2}^{-1} 1h_{11/2}^{-1} 2f_{7/2}$ with the purity gradually increasing ranging from $\simeq 82\%$ to 95% . The second $15/2_2^+$ state, although originates from the same partition has much less purity ($\simeq 61\%$). The $17/2_2^+$ evolves from $\nu 2d_{3/2}^{-1} 1h_{11/2}^{-1} 1h_{9/2}$ partition with 82% contribution.

The negative parity states $15/2_1^-$, $17/2_1^-$, $19/2_1^-$, $21/2_1^-$, and $23/2_1^-$ have more pure structure with 94%, 83%, 96%, 88% and 94% contributions, respectively, from the $\nu 1h_{11/2}^{-2} 2f_{7/2}$ partition. These states are compared with theory by considering the excitation energy of the $11/2_1^-$ isomer as zero.

6. $^{132}_{51}\text{Sb}_{81}$

This odd-odd isotope has one proton particle and one neutron hole with respect to the doubly closed ^{132}Sn .

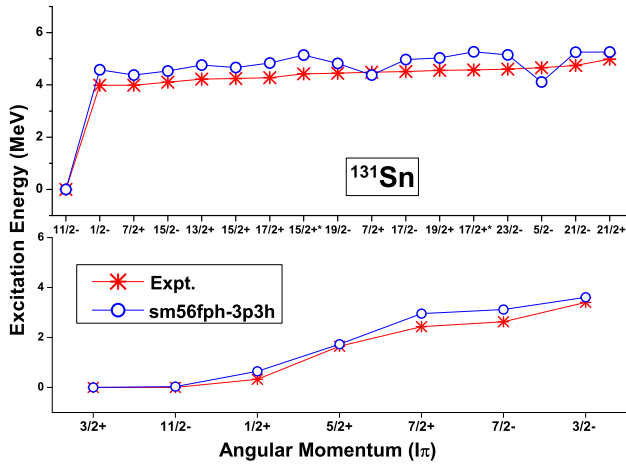


FIG. 8: Comparison of experimental spectra of ^{131}Sn with theory. More details are included in the legend, caption of Fig. 4 and the text.

At low excitation energies, the different states of this nucleus arise mainly from the interaction between the single proton and the single neutron hole. The experimental data have been reported in Refs. [28–30].

The 4^+ ground state and 3_1^+ state have been identified from earlier work to be composed of coupling between $\pi 1g_{7/2} - \nu 2d_{3/2}^{-1}$. The calculations reproduced the sequence as well the composition as per earlier reports (Fig. 9). The 3_1^+ state comes at an energy of 135 keV where the experimental energy is 85.55(6) keV. This state is also an isomer with a half-life of 15.62(13) ns.

The low lying 8_1^- isomer, whose experimental energy is yet to be determined has been produced at 193 keV in the calculations, with a dominant configuration as $\pi 1g_{7/2} - \nu 1h_{11/2}^{-1}$. This state is a beta decaying isomer having a half-life of 4.10(5) min. In the adopted levels [1], its excitation energy is not specified but it was predicted to be around 150-250 keV from the ground state [29]. In the atomic mass database [31], this level is specified at 200 keV with an uncertainty of 30 keV. The other members of this multiplet, $J = 3_1^-, 4_1^-, 6_1^-, 9_1^-$ are experimentally seen. In most of the cases, the purity of the structure is greater than 95%.

After 2.5 MeV, two positive parity states 10^+ , 11^+ states were observed from the fission of ^{248}Cm by P. Bhattacharyya *et al.* [32]. These two states were identified to originate from coupling of $\pi 1h_{11/2} - \nu 1h_{11/2}^{-1}$ with experimental energies 2.8 and 3.2 MeV, respectively. Because of absence of $\pi 1h_{11/2}$ orbit, we could not reproduce these states.

A few more positive (11^+ , 12^+ , 13^+) as well as negative (12^- , 13^- , 14^- , 15^-) parity levels were identified at excitation energies above 4 MeV. To generate spin more than 11, the core has to be excited i.e., one neutron has to be excited to the orbitals above the $N=82$

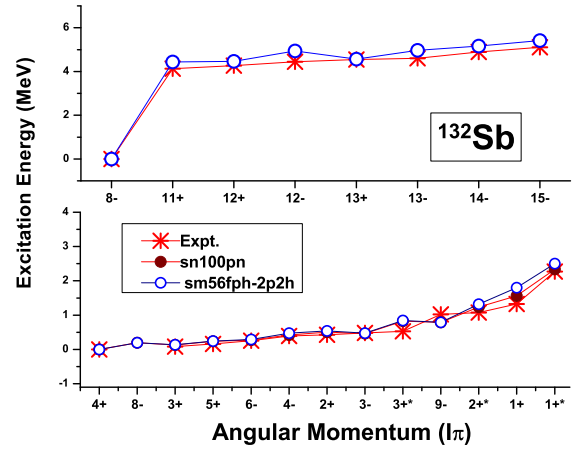


FIG. 9: Comparison of experimental spectra of ^{132}Sb with theory. More details are included in the legend, caption of Fig. 4 and the text.

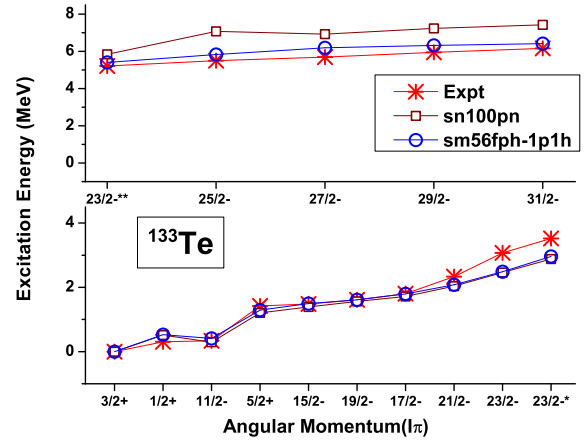


FIG. 10: Comparison of experimental spectra of ^{133}Te with theory. More details are included in the legend, caption of Fig. 4 and the text.

shell gap. These high spin states have been found to decay to the 8^- isomer, whose experimental energy is not known yet. Thus we have compared the experimental data with theoretical predictions considering the 8_1^- (theo) state (i.e. 193 keV) to be zero. The 11^+ state is member of the multiplet $\pi 1g_{7/2} - \nu 1h_{11/2}^{-1} 2d_{3/2}^{-1} 2f_{7/2}$ with 84% parentage. However, the other states 12^+ , 13^+ are coming from $\pi 1g_{7/2} - \nu 1h_{11/2}^{-1} 2d_{3/2}^{-1} 1h_{9/2}$ partition with 86% and 90% contributions. However, the core excited negative parity states (12^- to 15^-) have around 90-96% parentage from $\pi 1g_{7/2} - \nu 1h_{11/2}^{-2} 2f_{7/2}$ partition.

7. ${}^{133}_{52}\text{Te}_{81}$

${}^{133}\text{Te}$ can be described as ${}^{132}\text{Sn}$ with additional two protons and one neutron hole. The second excited state ($11/2^-$) at 0.334 MeV is a beta decaying isomer with $T_{1/2} = 55.4$ (4) min. It is theoretically predicted at 0.413 MeV. The experimental details of the $3/2^+$ ground state, the $1/2^+$ state below this isomer and other low-spin states have been found from β^- decay of ${}^{133}\text{Sb}$ [1].

The theoretical results are compared with experimental data in Fig. 10. The positive parity states $3/2_1^+$ and $5/2_1^+$ have contributions 93% and 74%, respectively, from the partition $\pi 1g_{7/2}^2 - \nu 2d_{3/2}^{-1}$. On the other hand, $1/2^+$ state is originated from the partition $\pi 1g_{7/2}^2 - \nu 3s_{1/2}^{-1}$ with 74% amplitude.

The yrast isomer $11/2^-$ and other members of the sequence $15/2_1^-$, $17/2_1^-$, $19/2_1^-$, $23/2_1^-$ originate from $\pi g_{7/2}^2$ coupled with $\nu h_{11/2}^{-1}$ with more than 90% contribution. The yrast $21/2^-$ has a mixed structure with 52% contribution from the partition $\pi g_{7/2}^2 - \nu h_{11/2}^{-1}$ and 46% from $\pi 1g_{7/2} 2d_{5/2} - \nu 1h_{11/2}^{-1}$. The $23/2_2^-$ state originates from $\pi 1g_{7/2} 2d_{5/2} - \nu 1h_{11/2}^{-1}$ (98%) as also suggested by Hwang *et al.* [33].

The positive states near 4 MeV, ($21/2^+$, $25/2^+$, $23/2^+$, $27/2^+$) are not reproduced well in the present calculations. Hwang *et al.* [33] have identified these states to originate from $\pi 1g_{7/2} 1h_{11/2} - \nu 1h_{11/2}^{-1}$. Thus these energies could not be reproduced in the present calculations because of the absence of the proton $1h_{11/2}$ orbit in the model space.

Hwang *et al.* [33] interpreted the sequence of states beginning at 5.2 MeV in ${}^{133}\text{Te}$ as originated from the particle-hole excitation from the ${}^{132}\text{Sn}$ core. From our calculation, the $23/2_3^-$ and $25/2_1^-$ have major contribution (86% and 71%, respectively) from the partition $\pi 1g_{7/2}^2 - \nu 1h_{11/2}^{-2} 2f_{7/2}^{-1}$. However, the other band members, *viz.*, $27/2_1^-$, $29/2_1^-$ and $31/2_1^-$ have contributions from both $\pi 1g_{7/2} 2d_{5/2} - \nu 1h_{11/2}^{-2} 2f_{7/2}^{-1}$ (61-75%) and $\pi 1g_{7/2}^2 - \nu 1h_{11/2}^{-2} 2f_{7/2}^{-1}$ (30-21%). As expected, the results with *sn100pn* interaction show substantial deviation from experimental data.

- Calculations for $N=83$ isotones

8. ${}^{134}_{51}\text{Sb}_{83}$

${}^{134}\text{Sb}$ can be characterised as one proton and one neutron particle outside the ${}^{132}\text{Sn}$ core. The Fig. 11 shows the comparison of theoretical results (done with *CWG* interaction and 1p1h and 2p2h excitations modes with *sm56fph* interaction) with experimental data. Both

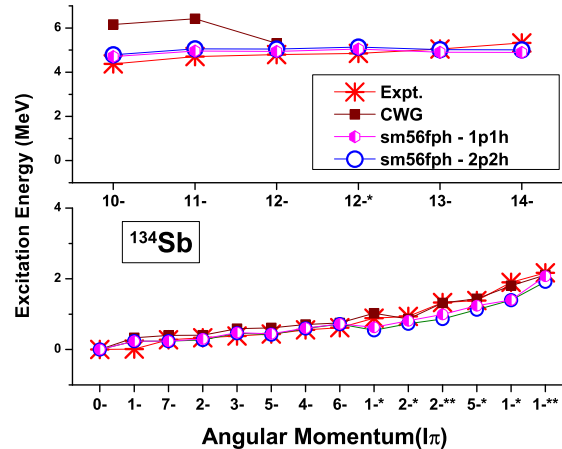


FIG. 11: Comparison of experimental spectra of ${}^{134}\text{Sb}$ with theory. More details are included in the legend, caption of Fig. 4 and the text.

the modes reproduce the experimental data for higher spin states much better than those predicted by *CWG*.

${}^{134}\text{Sb}$ has a beta decaying isomer with spin 7^- having $T_{1/2} = 10.07$ (5)s. The details of low lying structure have been obtained from β^- and β^-n decay of ${}^{134,135}\text{Sn}$, respectively [34]. There is an experimentally observed 1^- state almost degenerate to 0^- at 13 keV. Both *CWG* and *sm56fph* interactions are unable to reproduce the low-lying 1^- state. The yrast 0^- to 7^- states have dominant contribution of the partition $\pi 1g_{7/2} - \nu 2f_{7/2}$. The second 1^- state originates from the partition $\pi 1g_{7/2} - \nu 1h_{9/2}$. The 2_2^- and 2_3^- have around 70% contributions from $\pi 1g_{7/2}$ coupled with neutron in $1h_{9/2}$ and $3p_{3/2}$, respectively. The 5_2^- state has a leading contribution 59% from the partition $\pi 1g_{7/2} - \nu 3p_{3/2}$. Near 2 MeV, 1_3^- and 1_4^- have proton in $2d_{5/2}$ coupled with neutron in $2f_{7/2}$ (94%) and $3p_{3/2}$ (95%), respectively.

After 2 MeV, the positive states experimentally observed are 9^+ and 10^+ states which have dominant contribution from the partitions $\pi 1h_{11/2} - \nu 2f_{7/2}$ and $\pi 1g_{7/2} - \nu 1i_{13/2}$, respectively, as discussed in Ref. [35]. But, our calculation predict these states at higher energies because of unavailability of proton $1h_{11/2}$ and neutron $1i_{13/2}$ orbits in the model space.

The high spin negative parity states arise from the neutron core breaking. In our calculation in 2p2h mode, the yrast 10^- state has been reproduced with leading contribution (73%) from the partition $\pi 1g_{7/2} - \nu 1h_{11/2}^{-1} 2f_{7/2}^2$. The other negative parity yrast 11^- to 14^- states have gradually increasing contribution of the partition $\pi 1g_{7/2} - \nu 1h_{11/2}^{-1} 2f_{7/2} 1h_{9/2}$ ranging from 49% to 92%. This structure is different from that ($\pi 1g_{7/2} - \nu 1h_{11/2}^{-1} 2f_{7/2}^2$) suggested by Fornal *et al.* in Ref [35].

9. $^{135}_{52}\text{Te}_{83}$

^{135}Te consists of two protons and one neutron outside doubly magic ^{132}Sn . The low lying states of this nucleus were studied mainly from the beta decay studies by Hoff et al.[36]. The information about the isomeric state is known from Kawade et al.[37]. The investigation regarding the high spin states are known from Refs. [35, 38, 39]. The Fig. 12 shows the comparison of theoretical results (done with *CWG* interaction and 1p1h excitations mode with *sm56fp* and *sm56fph* interactions) with experimental data. Both the modes reproduce the experimental data for higher spin states much better than those predicted by *CWG*.

For *sm56fp*, low lying states ($7/2^-$, $11/2^-$, $15/2^-$) are originated from the partition $\pi 1g_{7/2}^2 - \nu 2f_{7/2}$ with contributions approximately 94, 91 and 82%, respectively. Same is observed for *sm56fph* with contributions approximately 93, 87 and 82%, respectively. The yrast $3/2^-$ state has 75% contribution of the partition $\pi 1g_{7/2}^2 - \nu 3p_{3/2}$ for *sm56fp* with and 73% for *sm56fph*. For $1/2^-$ and $5/2^-$ states, the dominant partition is $\pi 1g_{7/2}^2 - \nu 2f_{7/2}$ and it contributes 78% (77%) and 71% (65%), respectively, for *sm56fp* (*sm56fph*) interaction. For *sm56fph* interaction, the $9/2^-$ state has 95% contribution from the partition $\pi 1g_{7/2}^2 - \nu 2f_{7/2}$. However, this yrast state has 97% contribution from $\pi 1g_{7/2}^2 - \nu 2f_{7/2}$ for *sm56fp* interaction.

Yrast $19/2^-$ state originates from the partitions $\pi 1g_{7/2}^2 - \nu 2f_{7/2}$ with 47%(48%) and $\pi 1g_{7/2}^2 2d_{5/2} - \nu 2f_{7/2}$ with 53%(50%) contributions, for *sm56fp* (*sm56fph*) interaction. The second $19/2^-$ has $\pi 1g_{7/2}^2 - \nu 2f_{7/2}$ partition with 53%(50%) and $\pi 1g_{7/2}^2 2d_{5/2} - \nu 2f_{7/2}$ with 47%(48%) contribution for *sm56fp* (*sm56fph*) interaction. The $19/2_3^-$ has dominant contribution of 78% from the partition $\pi 1g_{7/2}^2 - \nu 1h_{11/2}^{-1} 2f_{7/2}^2$ for *sm56fp*. On the other hand, in case of *sm56fph* it has a contribution of 98% from $\pi 1g_{7/2}^2 - \nu 1h_{9/2}$ partition.

The yrast $21/2^-$ has 52% contribution from $\pi 1g_{7/2}^2 2d_{5/2} - \nu 1h_{11/2}^{-1} 2f_{7/2}^2$ partition, in case of *sm56fp* interaction. But for *sm56fph* interaction the dominant contribution is coming from $\pi 1g_{7/2}^2 - \nu 1h_{9/2}$ (86%). The $21/2_2^-$ state has $\pi 1g_{7/2}^2 - \nu 1h_{11/2}^{-1} 2f_{7/2}^2$ with 52% along with competing contribution of 36% from $\pi 1g_{7/2}^2 2d_{5/2} - \nu 1h_{11/2}^{-1} 2f_{7/2}^2$ for *sm56fp*. For *sm56fph*, this state mainly arises from $\pi 1g_{7/2}^2 2d_{5/2} - \nu 1h_{9/2}$ with 86% contribution.

The $23/2_1^-$, $25/2_1^-$, $27/2_1^-$, $29/2_1^-$, $31/2_1^-$, $33/2_1^-$ and $35/2_1^-$ states have contributions from $\pi 1g_{7/2}^2 - \nu 1h_{11/2}^{-1} 2f_{7/2}^2$ and $\pi 1g_{7/2}^2 2d_{5/2} - \nu 1h_{11/2}^{-1} 2f_{7/2}^2$ with amplitudes ranging from 41% - 13% and 31% - 86% for *sm56fp* interaction.

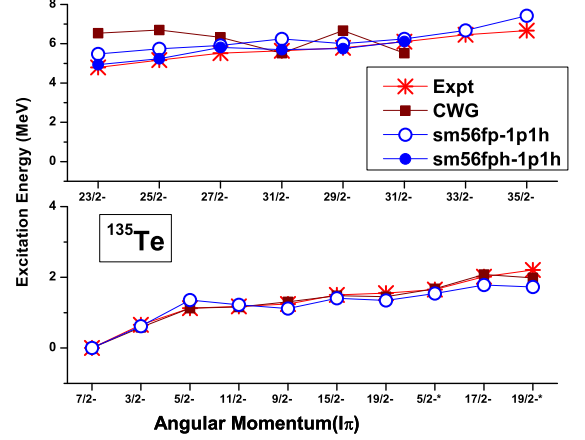


FIG. 12: Comparison of experimental spectra of ^{135}Te with theory. More details are included in the legend, caption of Fig. 4 and the text.

For *sm56fph* interaction, $23/2_1^-$, $25/2_1^-$, $27/2_1^-$, $29/2_1^-$, $31/2_1^-$, $33/2_1^-$ and $35/2_1^-$ have a mixed structure of partitions $\pi 1g_{7/2}^2 - \nu 1h_{11/2}^{-1} 2f_{7/2} 1h_{9/2}$ and $\pi 1g_{7/2}^2 2d_{5/2} - \nu 1h_{11/2}^{-1} 2f_{7/2} 1h_{9/2}$ with amplitudes ranging from 86%-25% and 2-74%.

Some of the positive parity states (say, $21/2^+$, $25/2^+$, $27/2^+$ etc.) could not be reproduced well with these two interactions because of absence of proton $h_{11/2}$ orbital in the model space.

C. Transition Probabilities in ^{132}Sn and its neighbours

The transition probabilities of yrast states which arise from cross-shell excitations in ^{132}Sn , ^{131}Sn , ^{133}Sb and ^{134}Te isotopes, for which experimental data [1] are available, have been calculated (Table I) for *sm56fph* and compared with experimental data [1]. In case of $E\lambda$ ($\lambda=2-4$) the neutron effective charge is taken as $1.2e$. The results for all modes of excitation, which were calculated are shown in the table. However, the results for different modes are almost similar.

The results reproduce data reasonably well for ^{132}Sn , except in a few cases (8^+ to 6^+ and those involving the 3^- state). For magnetic transitions, quenched intrinsic neutron g-factor (g_n^s) by a factor of 0.7, improves the results.

Gross mismatch is observed for the $E3$ transition rate from the 3_1^- state. It has been already discussed that this state possibly has a collective structure and thus its energy as well as transition rates are not reproduced in this calculation with such limited options for excitations.

In case of $E1$ transition, effective charge has been taken as $e_n^{eff} = 0.35e$ and $e_p^{eff} = 1.64e$ (Table I). However,

the calculated values are underestimated compared to experimental data by one order of magnitude in most cases. However for E1 transitions from $5_1^- \rightarrow 4^+$ state, the $B(E1)$ values are well reproduced. The $B(E1)$ value for $5_1^- \rightarrow 6^+$ state is overpredicted compared to experimental data.

The $2f_{5/2}$, $3p_{1/2}$, and $1i_{13/2}$ orbits have been excluded from the model space. They are not usually significant for reproduction of energy eigenvalues or transition probabilities of the nuclei which are being discussed in this work. However this argument does not hold for E1 transition probabilities, *i.e.* for $B(E1)$ values. These transitions occur due to (very) small contributions of the orbitals originating in higher shells in the wavefunction. Thus small overlap in wave-functions are also significant for proper reproduction of experimental $B(E1)$ s, which are always at least 5-6 orders of magnitude slower than the single particle estimate.

For ^{131}Sn , the $B(E2)$ value for the $23/2^-$ to $19/2^-$ transition has been reproduced with the same effective charge to a reasonable extent. However, the $B(E1)$ and $B(E4)$ values are under-predicted.

For ^{133}Sb , the sharp difference between experimental $B(M1)$ values extracted for the $15/2^+ \rightarrow 13/2^+$ and $13/2^+ \rightarrow 11/2^+$ transitions could not be reproduced for the calculated yrast states for both $1p1h$ and $2p2h$ modes. However, $2p2h$ mode reproduces their energies quite well. This is similar to the observation of Wang *et al.* [2]. However, the calculated $B(E2)$ value of the $21/2^+ \rightarrow 17/2^+$ transition from the microsecond $21/2^+$

isomer (without the internal conversion correction) also yields a milli-second half life of the isomer as reported by B. Sun *et al.* [17].

In ^{134}Te , calculated $B(E2)$ for the core excited 12^+ is under-predicted in theory.

IV. SUMMARY AND CONCLUSION

The excitation spectra of ^{132}Sn and its nearest neighbours have been reproduced with a new cross-shell interaction. A few two body matrix elements have been tuned to reproduce the low-lying multiplet states of ^{132}Sn . This is the first full scale shell model study of ^{132}Sn energy spectra as well as transition probabilities. The excitation spectra for other nearest neighbours are reproduced well. The transition probabilities of core-excited states are also reproduced reasonably well. The most important observable calculated are the E1 transition probabilities for nuclei below and above ^{132}Sn . Interestingly, the $B(E1)$ rates from 5_1^- state in ^{132}Sn are reproduced reasonably well. However, other calculated $B(E1)$ values are systematically underpredicted. It indicates the need for inclusion of other higher energy neutron orbits in the model space. The new interaction will have far reaching consequences in explaining low -lying E1 isomers in mid-shell Sn and other nuclei with $N < 82$ as well in those beyond $N=82$.

-
- [1] <https://www.nndc.bnl.gov/>
- [2] H.-K. Wang, S. K. Ghorui, K. Kaneko, Y. Sun, Z. H. Li, *Phys. Rev. C* **96**, 054313 (2017).
- [3] B.A. Brown, N. J. Stone, J. R. Stone, I. S. Towner, M. Hjorth-Jensen, *Phys. Rev. C* **71**, 044317 (2005).
- [4] Kris L. G. Heyde, in *The Nuclear Shell Model*, (Springer, Heidelberg, 1990) pp. 375.
- [5] P. Bhattacharyya, P. J. Daly, C. T. Zhang, Z. W. Grabowski, S. K. Saha, R. Broda *et al.*, *Phys. Rev. Lett.* **87**, 062502 (2001).
- [6] G. Bocchi, S. Leoni, B. Fornal, G. Colò, P.F. Bortignon, S. Bottoni *et al.*, *Phys. Lett. B* **760**, 273 (2016).
- [7] O. Sorlin, M. -G. Porquet, *Prog. Par. Nucl. Phys.* **61**, 602 (2008).
- [8] G. Audi, W. Meng, *Atomic Mass Evaluation 2013: Private Communication April 2011*.
- [9] B.A. Brown, W.D. M. Rae, *Nucl. Data sheets* **120**, 115 (2014).
- [10] B. A. Brown, A. Etchegoyen, N. S. Godwin, W. D. M. Rae, W. A. Richter, W. E. Ormand, E. K. Warburton, J. S. Winfield, L. Zhao and C. H. Zimmerman, MSU-NSCL report number **1289** (2004).
- [11] B. Fogelberg, M. Hellström, D. Jerrestam, H. Mach, J. Blomqvist, A. Kerek, L. O. Norlin, and J. P. Omtvedt, *Phys. Rev. Lett.* **73**, 2413 (1994).
- [12] S. Borg, G.B. Holm and B. Rydberg, *Nucl. Phys. A* **212**, 197 (1973).
- [13] K. Sistemich, W. -D. Lauppe, T. A. Khan, H. Lawin, H. A. Selič, J. P. Bocquet, E. Monnard, F. Schussler, *Z. Phys. A* **285**, 305 (1978).
- [14] W. Urban, W. Kurcewicz, A. Korgul, P. J. Daly, P. Bhattacharyya, C. T. Zhang *et al.*, *Phys. Rev. C* **62**, 027301 (2000); W. Urban, A. Złomaniec, G. S. Simpson, H. Faust, T. Rzaca-Urban, M. Jentschel, *ibid* **79**, 037304 (2009).
- [15] J. Blomqvist, A. Kerek, B. Fogelberg, *Z. Phys. A* **314**, 199 (1983).
- [16] J. Genevey, J.A. Pinston, H. Faust, C. Foin, S. Oberstedt and B. Weiss, *Eur. Phys. J. A* **7**, 463 (2000).
- [17] B. Sun, R. Knöbel, H. Geissel, Yu.A. Litvinov, P.M. Walker, K. Blaum *et al.*, *Phys. Lett. B* **688**, 294 (2010).
- [18] B. Fogelberg, B. Ekström, L. Sihver, G. Rudstam, *Phys. Rev. C* **41**, R1890 (1990).
- [19] J. P. Omtvedt, H. Mach, B. Fogelberg, D. Jerrestam, M. Hellström, L. Spanier, K. I. Erokhina, and V. I. Isakov, *Phys. Rev. Lett.* **75**, 3090 (1995).
- [20] C. T. Zhang, P. Bhattacharyya, P. J. Daly, R. Broda, Z. W. Grabowski, D. Nisius *et al.*, *Phys. Rev. Lett.* **77**, 3743 (1996).
- [21] P.J. Daly, C.T. Zhang, P. Bhattacharyya, R. Broda, Z.W. Grabowski, D. Nisius *et al.*, *Z. Phys. A* **358**, 203 (1997).
- [22] S. K. Saha, C. Constantinescu, P. J. Daly, P. Bhattacharyya, C. T. Zhang, Z. W. Grabowski *et al.*, *Phys. Rev. C* **65**, 017302 (2001).

TABLE I: The comparison of theoretical transition rates of yrast states which arise from cross-shell excitations in ^{132}Sn , ^{131}Sn , ^{133}Sb and ^{134}Te isotope with experimental data [1]. The B(M1) values are quoted in μ_n^2 . The B(E λ) values are quoted in unit of $e^2 fm^{2\lambda}$. The B(E1) values are quoted in the unit of $10^{-6} e^2 fm^2$.

Nucleus	J_i	J_f	E_γ (keV)	Type	Expt. (Error)	Effective charges		Theory		
						e_p	e_n	1p1h	Mode 2p2h	3p3h
^{132}Sn										
	2 ⁺	0 ⁺	4041.1	E2	224.6 (6)	-	1.2	235.3	232.8	232.9
	4 ⁺	2 ⁺	375.1	E2	16.3 (10)	-	"	3.4	3.3	3.0
	6 ⁺	4 ⁺	299.6	E2	11.9 (4)	-	"	8.1	8.3	8.0
	8 ⁺	6 ⁺	132.5	E2	4.2 (1)	-	"	0.49	0.48	0.26
	5 ⁻	3 ⁻	590.6	E2	24.9(3)	-	"	0.09	0.041	0.05
	3 ⁻	0 ⁺	4351.9	E3	>7348.4	-	1.2	82.3	81.5	71.5
	4 ⁺	0 ⁺	4416.2	E4	227.1(4) $\times 10^3$	-	1.2	153 $\times 10^3$	154 $\times 10^3$	149 $\times 10^3$
	3 ⁻	2 ⁺	310.7	E1	> 284	1.64	0.35	-	0.31	0.83
	4 ⁺	3 ⁻	64.4	E1	4.45(55)	"	"	-	0.055	0.12
	4 ⁻	4 ⁺	414.6	E1	4.85(48)	"	"	-	0.29	0.23
	5 ⁻	6 ⁺	226.7	E1	4.90(53)	"	"	-	25.3	26.4
	5 ⁻	4 ⁺	526.2	E1	140(15)	"	"	-	113.8	120.1
	7 ⁺	8 ⁺	70.4	M1	0.042(5)			0.019	0.034	0.033
	7 ⁺	6 ⁺	203.1	M1	0.066(7)			0.029	0.046	0.045
	5 ⁻	4 ⁻	111.5	M1	0.123(14)			0.028	0.023	0.020
^{131}Sn										
	19/2 ⁻	17/2 ⁺	173.185	E1	> 333	1.64	0.35	-	0.13	0.40
	23/2 ⁻	19/2 ⁻	158.50	E2	14.7 (10)	-	1.2	9.43	9.60	9.1
	19/2 ⁻	11/2 ⁻	4446.0	E4	> 1.891 $\times 10^6$	-	1.2	1.069 $\times 10^5$	1.078 $\times 10^5$	1.03 $\times 10^5$
^{133}Sb										
	21/2 ⁺	17/2 ⁺	< 20	E2	~ 10.48	1.85	0.35	1.16	1.17	-
	15/2 ⁺	13/2 ⁺	162.3	M1	> 0.43		free g ^s	0.19	0.17	-
	13/2 ⁺	11/2 ⁺	110.2	M1	0.0075 (27)		"	0.58	0.61	-
^{134}Te										
	12 ⁺	10 ⁺	182.6	E2	133 (12)	2.0	0.0	36.8	41.1	-

- [23] M. Samri, G. J. Costa, G. Klotz, D. Magnac, R. Seltz and J. P. Zirnheld, Z. Phys. A **321**, 255 (1985).
- [24] L. -E. De Geer, G. B. Holm, Phys. Rev. C **22**, 2163 (1980).
- [25] B. Fogelberg, J. Blomqvist, Phys. Rev. Lett. B **137**, 20(1984).
- [26] B. Fogelberg, J. Blomqvist, Nucl. Phys. A. **429**, 205 (1984).
- [27] B. Fogelberg, H. Gausemel, K. A. Mezilev, P. Hoff, H. Mach, M. Sanchez-Vega *et al.*, Phys. Rev. C **70**, 034312 (2004).
- [28] A. Kerek, G.B. Holm, P. Carlé, J. McDonald, Nucl. Phys. A. **195**, 159 (1972).
- [29] C.A. Stone, S. H. Faller, W. B. Walters, Phys. Rev. C **39**, 1963 (1989).
- [30] H. Mach, D. Jerrestam, B. Fogelberg, M. Hellström, J. P. Omtvedt, K. I. Erokhina, V. I. Isakov, Phys. Rev. C **51**, 500 (1995).
- [31] G. Audi, O. Bersillon, J. Blachot, A.H. Wapstra, Nucl. Phys. A. **729**, 3 (2003).
- [32] P. Bhattacharyya, P. J. Daly, C. T. Zhang, Z. W. Grabowski, S. K. Saha, B. Fornal *et al.*, Phys. Rev. C **64**, 054312 (2001).
- [33] J. K. Hwang, A. V. Ramayya, J. H. Hamilton, C. J. Beyer, J. O. Rasmussen, Y. X. Luo *et al.*, Phys. Rev. C. **65**, 034319 (2002).
- [34] J. Shergur, A. Wöhr, W. B. Walters, K.-L. Kratz, O.

- Arndt, B. A. Brown *et al.*, Phys. Rev. C. **71**, 064321 (2005).
- [35] B. Fornal, R. Broda, P. J. Daly, P. Bhattacharyya, C. T. Zhang, Z. W. Grabowski *et al.*, Phys. Rev. C **63**, 024322 (2001).
- [36] P. Hoff, B. Ekström, B. Fogelberg, Z. Phys. A. **332**, 407 (1989).
- [37] K. Kawade, G. Battistuzzi, H. Lawin, K. Sistemich, J. Blomqvist, Z. Phys. A. **298**, 273 (1980).
- [38] P. Bhattacharyya, C. T. Zhang, B. Fornal, P. J. Daly, Z. W. Grabowski, I. Ahmad *et al.*, Phys. Rev. C **56**, R2363(R) (1997).
- [39] Y. X. Luo, J. O. Rasmussen, A. V. Ramayya, J. H. Hamilton, X. Q. Zhang, J. K. Hwang *et al.*, Phys. Rev. C **64**, 054306 (2001).